frontiers | Frontiers in Environmental Science

TYPE Original Research
PUBLISHED 01 October 2025
DOI 10.3389/fenvs.2025.1675720

OPEN ACCESS

EDITED BY
Marco Contin,
University of Udine, Italy

REVIEWED BY
Deepanjali Gupta,
G. B. Pant University of Agriculture and Technology, India
Vivek Ghimirey,
Agriculture and Forestry University, Nepal
Alexander Craig,
Uppsala University, Sweden

*CORRESPONDENCE
Livia V. C. Charamba,
livia.charamba@tu-dresden.de

RECEIVED 29 July 2025
ACCEPTED 12 September 2025
PUBLISHED 01 October 2025

CITATION
Charamba LVC, Houska T, Kaiser K, Knorr K-H, Krause T, Chen H, Krám P, Hruška J, Müller I and Kalbitz K (2025) The deeper, the more distinct: dissolved organic matter composition differs between soil types and diverges with depths. *Front. Environ. Sci.* 13:1675720. doi: 10.3389/fenvs.2025.1675720

The deeper, the more distinct: dissolved organic matter composition differs between soil types and diverges with depths

Livia V. C. Charamba[1]*, Tobias Houska[1,2], Klaus Kaiser[3], Klaus-Holger Knorr[4], Tobias Krause[1], Huan Chen[5], Pavel Krám[6,7], Jakub Hruška[6,7], Ingo Müller[8] and Karsten Kalbitz[1]

[1]Department of Forest Sciences, Institute of Soil Science and Site Ecology, TUD Dresden University of Technology, Tharandt, Germany, [2]Department of Landscape Ecology and Resource Management, Justus Liebig University, Gießen, Germany, [3]Soil Science and Soil Protection, Martin Luther University Halle-Wittenberg, Halle (Saale), Germany, [4]Institute for Landscape Ecology, Ecohydrology and Biogeochemistry Group, University of Münster, Münster, Germany, [5]Department of Environmental Engineering and Earth Science, Clemson University, Clemson, SC, United States, [6]Czech Geological Survey, Prague, Czechia, [7]Global Change Research Institute of the Czech Academy of Sciences, Brno, Czechia, [8]Saxon State Office for Environment, Agriculture and Geology, Freiberg, Germany

Dissolved organic matter (DOM) is a key component in the carbon and energy cycling of soil and aquatic ecosystems. Tracking DOM composition through soil profiles provides insight into the processes driving its transport and transformation. However, there is a lack of studies investigating whether DOM composition in deeper mineral soil is driven by topsoil inputs, or if processes during soil passage cause a rather uniform DOM quality irrespective of the source. Understanding the topsoil influence on subsoil DOM and depth-dependent transformation patterns is crucial for the transfer to and its fate within aquatic ecosystems. To address this knowledge gap, we examined the compositional features of DOM sampled in situ along depth profiles of four contrasting soil types (Peat, peaty Gleysol, Cambisol, Podzol) in a mountainous catchment (Ore Mountains, Germany). A combination of pyrolysis-gas chromatography/mass spectrometry and UV and fluorescence spectroscopy was used to characterize the molecular properties of DOM and similarities across the different soils and depths were achieved by Bray-Curtis dissimilarity analysis. Results revealed site-specific decreases in similarity with depth, driven by soil processes that progressively alter DOM composition. In Peat, composition remained rather similar between D1 and D2 or D3 (57-59%), likely due to constantly anoxic conditions that inhibit oxidative degradation and transformation of DOM. In the peaty Gleysol, moderate transformations were observed (41-59% similarity), likely driven by alternating redox conditions and sorptive interactions. The strongest compositional changes occurred in the Cambisol with similarity between D1 and D3 reaching 18%, suggesting microbial processing in conjunction with sorptive interactions with the mineral phase. In the Podzol, the formation of organo-metal complexes promoted selective preservation of aromatic structures. The site-specific processes led to decreases in both the number and abundance of identified shared compounds with depth, contrasting the assumption of DOM similarity across different soil types. Despite the changes with depth, subsoil DOM composition in Peat, peaty Gleysol, and Podzol still retained some imprint of topsoil sources. This study

highlights how site-specific biotic and abiotic processing generates unique DOM composition that shape organic matter cycling in soils and its ecological implications in aquatic systems.

KEYWORDS

dissolved organic matter, cross-site similarities, horizontal variability, pyrolysis-gas chromatography/mass spectrometry, fluorescence spectroscopy, uniform DOM composition

1 Introduction

Dissolved organic matter (DOM) is a mixture of dissolved and colloidally dispersed (<0.45 μm) organic compounds present throughout the terrestrial and aquatic ecosystems. While it may be derived from soil organic matter (SOM) (Steinbeiss et al., 2008; Kalbitz et al., 2000), or from microbial necromass (Nannipieri et al., 2025; Sokol and Bradford, 2019), DOM can also originate from recent aboveground litter, root and microbial exudates (De Troyer et al., 2011). Being the most mobile fraction of organic matter, it plays a critical role in the biogeochemical cycles along the terrestrial-aquatic continuum. DOM has a complex composition, including components identified as aliphatic and aromatic compounds, phenols, carbohydrates, sugars, proteins, amino acids, nucleic acids, and lipids (Pontiller et al., 2020). Its composition and reactivity vary across environmental compartments and are influenced by factors such as land use, human impact, soil type, depth, vegetation, and climate (Xenopoulos et al., 2021; Tong et al., 2021; Singh et al., 2017).

DOM undergoes significant changes as it moves through soil profiles, with its composition, concentration, and molecular structure evolving in response to various transformation and sorption processes. Biodegradability is an important factor, as microbial communities can utilize DOM compounds as sources of carbon and energy (Kellerman et al., 2015; Kalbitz et al., 2003). Selective microbial processing generates distinct vertical patterns in DOM composition, often leading to the progressive depletion of relatively labile components while more recalcitrant compounds residually enrich. In addition, sorption continuously modifies DOM composition along flow pathways via interactions with mineral surfaces (Kalbitz et al., 2005). Sorption is compound-selective and is based on properties such as aromaticity, functional groups, and molecular weight (Feng et al., 2005). Sorption, therefore, not only alters DOM composition directly but can also protect certain compounds from microbial degradation (Kleber et al., 2015). The formation of soluble organo-metal complexes, especially with iron and aluminum, further modifies DOM mobility and bioavailability, with complexation rates affected by pH, redox state, and competing cations (Xu and Tsang, 2024; Yang et al., 2024; Roberts et al., 2005). Under certain conditions, many of these complexes are insoluble, leading to precipitation and accumulation in specific soil horizons (Krettek and Rennert, 2021; Wagai et al., 2020). During periods of water saturation, reduced oxygen availability may limit microbial degradation of certain compounds, thereby promoting the preservation also of potentially labile DOM components (Roth et al., 2019). Moreover, hydrological flow conditions influence the balance between biological and sorptive processes, affecting DOM transformation during the soil passage. The overall residence time of water at different soil depths plays a critical role in determining the type and extent of DOM alteration. Thus, understanding how DOM composition is affected by these transformations along soil profiles is crucial for linking soil DOM with aquatic systems and for predicting DOM mobility, persistence, and ecological impacts across terrestrial-aquatic interfaces.

Despite extensive research on DOM in soil extracts (Seifert et al., 2016; Qin et al., 2020; Jiang et al., 2017; Lin et al., 2023; Zhang et al., 2019) and soil water (Charamba et al., 2024), the processes that govern DOM compositional changes along soil depth remain poorly understood (Meng et al., 2024; Roth et al., 2019; Kaiser et al., 2004). For example, Kalbitz et al. (2005) and Roth et al. (2019) reported an overall decline in aromatic structures (i.e., plant-derived compounds) and an increase in microbially-derived compounds

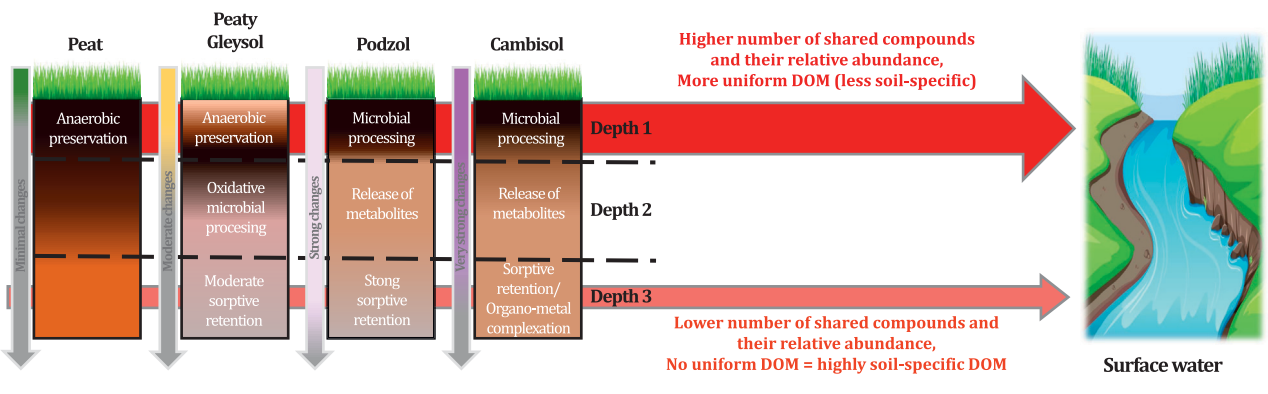

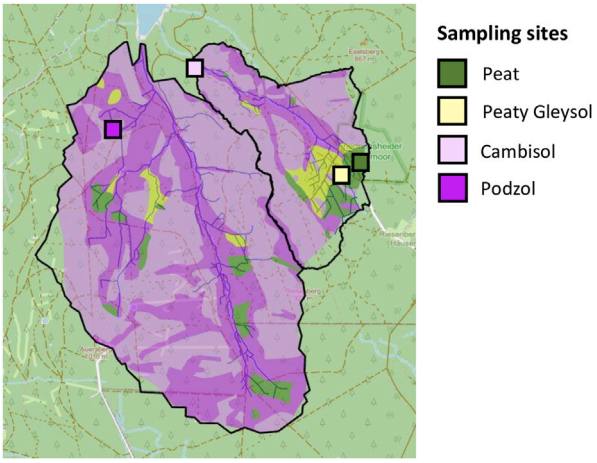

FIGURE 1
Map of the catchment area of the Sosa drinking water reservoir in the Ore Mountains (Germany). The sampling sites are indicated by squares, indicating also the soil type. The color scheme on the map illustrates the soil type distribution along the catchment area, Peat represented by green, peaty Gleysol by light-yellow, Cambisol by lilac, and Podzol by purple, which matches the color of the sampling sites.

with depth. Such findings could suggest a rater similar DOM composition at the deeper soil across different soil types. However, organic topsoil inputs, shaped by local vegetation, microbial communities, and varying stages of decomposition (Liu et al., 2021; O'Donnell et al., 2016), play a significant role in determining DOM composition in the topsoil. This initial heterogeneity is further changed by sorption, biodegradation, and leaching processes during downward relocation. Only few studies have addressed how these transformations influence DOM composition in deeper soil horizons, and their results remain contradictory. Davenport et al. (2023) reported that the composition of SOM as a main DOM source diverged across sites in deeper soil horizons. However, Freeman et al. (2024) observed that DOM became more similar with depth due to the accumulation of the persistent compounds. These contrasting observations highlight the fact that it remains unclear how strongly pedogenic processes shape differences in DOM composition in deeper soil horizons across different soil types, and how much of the topsoil DOM fingerprint persists in deeper horizons. This raises a fundamental question: does DOM composition tend toward uniformity with increasing soil depth?

To fill this knowledge gap, it is essential to apply robust and sensitive analytical techniques that can provide a comprehensive overview of the compounds present in DOM (Nebbioso and Piccolo, 2013). Both pyrolysis-gas chromatography/mass spectrometry, Py-GC/MS (Charamba et al., 2024; Jiang, er al., 2017), and fluorescence spectroscopy (Hua et al., 2023; Xue et al., 2013; Cannavo et al., 2004; Weishaar et al., 2003) are complementary and were proven to be sufficiently sensitive to track DOM compositional changes in natural environments (Gabor et al., 2014).

The aim of this study was to investigate the potential factors and processes influencing the variability and similarity of DOM composition across different soil types at different depths in the catchment of a drinking water reservoir in the Ore Mountains, Germany. Four sites, each dominated by a different soil type (Peat, peaty Gleysol, Cambisol, Podzol), were assessed to evaluate the variability of DOM composition with soil depth. We hypothesized that 1) similarity in DOM composition decreases with depth within individual soil profiles, driven by distinct microbial processing and abiotic interactions such as sorption to minerals, and 2) DOM composition in the deepest mineral soil horizons becomes more similar across soil types due to the relative accumulation of uniform, non-sorptive, and persistent compounds, although some compositional signatures from the overlying organic horizons likely remain. To test these hypotheses, we employed a combined approach of Py-GC/MS with a semi-automated compound identification pipeline (built in R version 4.4.1; R Core Team, 2024) that incorporated the National Institute of Standards and Technology (NIST) Mass Spectral Search 2.0, along with fluorescence spectroscopy. This enabled DOM characterization in soil water collected from three depths across the four soil types, hence allowing the comparison of DOM processing patterns within and among the soils.

2 Materials and methods

2.1 Study site and sampling

Soil water samples were collected biweekly (from winter 2020/2021 to spring 2022) at four different locations within the forested catchment area of the Sosa drinking water reservoir (Figure 1, Ore Mountains, Germany, 50°28′N 12°39′E). The catchment is in an area under a temperate climate, with an average annual temperature of 7.7 °C and an average annual precipitation of 1,133 mm. Most stands are composed of a variable mixtures of Norway spruce (*Picea abies*), European beech (*Fagus sylvatica*), and Silver fir (*Abies alba*), and few stands also feature Black alder (*Alnus glutinosa*).

The distribution of soil within the catchment is illustrated in Figure 1. Peat (i.e., Hemic Drainic Histosol; WRB, 2014) is mainly shallow, partially drained bogs with the upper 20 cm showing indications of enhanced oxidative decomposition and also comprises sites with the peats extending to 8 m depth. Peaty Gleysols feature shallow peat layers overlying wet mineral material layers and have been classified as Histic Dystric Gleysol (IUSS Working Group WRB, 2022). Most of the catchment area has mineral soils, mainly Dystric Cambisols and Carbic Entic Stagnic Podzols. Detailed information on soils in terms of their horizons, pH, TOC, C/N ratio, and soil texture is given in the Supplementary Material.

The monitoring system and sampling design for soil water was as outlined in Charamba et al., 2024: soil water was collected biweekly over a period of approximately 24 months at three different depths using suction plates and cups, following the International Cooperative Programme on Assessment and Monitoring of Air Pollution Effects on Forests (ICP Forests; http://icp-forests.net/; Nieminen et al., 2016) in Europe. The suction plates were installed below the organic layer overlying mineral soils or under the uppermost layer of Peat, where higher degradation was observed. To differentiate organic and mineral horizons, suction cups were installed in the upper and deeper

TABLE 1 Installation details of soil water sampling equipment (suction plates and cups) at different depths (D1, D2 and D3) across four soil types (Peat, peaty Gleysol, Cambisol, and Podzol). Horizon designations and their respective depths are detailed in the Supplementary Material.

Depth	Equipment installed	Site	Horizon where the suction plate/cup were installed	Depth installed
D1	Suction plate	Peat and peaty Gleysol	Underneath the uppermost organic horizon: Peat (Had) and peaty Gleysol (Al)	0 cm
		Cambisol and Podzol	Underneath the forest floor for Cambisol (Oe horizon) and Podzol (Oa horizon)	
D2	Suction cup	Peat	He	50 cm
		Peaty Gleysol	2Bl-Bg	45 cm
		Cambisol	2Bw	25 cm
		Podzol	2Bs	25 cm
D3	Suction cup	Peat	He	100 cm
		Peaty Gleysol	4Bl	80 cm
		Cambisol	3C	65 cm
		Podzol	4Bg	75 cm

mineral subsoil horizons, highlighting different pedogenic developments. For the Peat, the suctions cups were installed in two histic horizons. Further details on the horizons and depth where the suction plates and cups were installed are available in Table 1. Borosilicate glass suction plates and cups with a pore size of 1 µm were used to minimize DOM adsorption. Soil water was extracted using a continuous vacuum of 300 mbar. The same sampling setup, i.e., one suction plate and two suction cups, was repeated five times at each soil type/site.

Filtering of the soil solutions during the collecting with the suction plates and cups was effective, eliminating the need for additional filtration in the laboratory. Samples were stored in the refrigerator if measured on the following day, or in the freezer if analysis was carried out on a later day.

2.2 Sample preparation and laboratory analyses

2.2.1 Dissolved organic carbon (DOC), total nitrogen (TNb), nitrate-N + nitrite-N and ammonium-N

Samples were analyzed for concentrations of DOC and TNb using a Vario TOC cube (Elementar Analysensysteme GmbH, Langenselbold, Germany). To remove inorganic carbon, the samples were acidified to pH 1.8–2.0 using 37% HCl (Merck KGaA, Germany), and then 2.5 mL was injected into the analyzer for catalytic combustion with O_2 at 850 °C. An IR detector was employed to quantify the CO_2 released by the combustion process and a chemiluminescence detector (Horiba APNA-370) to measure the N release. The analytical error was ±0.25 mg L^{-1} for DOC and ±0.015 mg L^{-1} for TN.

Ammonium-N and nitrate-N + nitrite-N were measured by a AQ400 Discrete Analyzer (SEAL Analytical, Norderstedt, Germany) according to ISO/DIS 15923-1:2013 guidelines. The analytical error was ±0.015 mg L^{-1} for nitrate-N + nitrite-N and ±0.005 mg N L^{-1} for ammonium-N, respectively. Dissolved organic nitrogen (DON) was calculated by subtracting the sum of ammonium-N, nitrate-N and nitrite-N from the TN concentration.

2.2.2 Pyrolysis gas-chromatography/mass spectrometry (Py-GC/MS)

Composite samples were created by combining soil solutions from all five replicated sampling depths per monitoring site and sampling date. When sample volumes were insufficient for full analysis, two or a maximum of three composite samples from consecutive sampling dates were pooled. All the composite samples were kept frozen until freeze-drying. The freeze-dried samples were finely ground and stored in a desiccator to avoid moistening prior to analysis. The Py-GC/MS analysis did not include samples from spring 2021 due to technical constraints.

The freeze-dried composite samples were subsequently analyzed using pyrolysis-gas chromatography/mass spectrometry (Py-GC/MS). Prior to the analysis, 2 µL of androstane at a concentration of 37–81 µg L^{-1} (Sigma-Aldrich, St. Louis, MO, United States) was added to the samples (700 µg) as an internal standard. The samples underwent pyrolysis by a Multi-Shot Pyrolyzer EGA/PY-3030D (Frontier Laboratories Ltd.; Fukushima, Japan). The temperature for the pyrolytic process was set at 600 °C for 6s. The compounds released by the pyrolytic process were transported into the gas chromatograph (GC) (7890B GC, Agilent Technologies, Inc.; Santa Clara, CA, United States). A split injection (split ratio 1:20) was applied and helium was used as carrier gas at a flow rate of 1 mL min^{-1}. The inlet temperature of the gas chromatograph was set at 250 °C. The volatile compounds were separated using a Zebron ZB-5ms column (30 m length, 0.25 mm inner diameter, 0.25 µm film thickness). The temperature gradient employed was the following: initial temperature set at 50 °C, then increased to 300 °C at a rate of 7 °C min^{-1}, and then held at 300 °C for 10 min. The GC was coupled with a mass spectrometer detector (MSD, Agilent 5,977) with electron ionization of 70 eV and a mass detection range of 50–600 m/z, allowing for the identification of DOM pyrolysates produced through thermal decomposition of the original compounds. A semi-automated process to identify the peaks and

their quantification was used based on the methodology described in Chen et al. (2018) and Charamba et al. (2024).

The Py-GC/MS data was converted and then imported into the pipeline built in R version 4.4.1 (R Core Team, 2024), where the identification of chemical compounds through NIST Mass Spectral Search 2.0 was accomplished. Finally, all identified compounds were categorized into compounds groups according to their elemental composition and functional moieties. A final compound list with their chemical name, Chemical Abstracts Service Registry Number (CASRN), formula, molecular weight, and Simplified Molecular Input Line Entry System (SMILES), as well as major fragment ions was created.

Compound classification was performed as follows: aromatic hydrocarbons (ArH) are hydrocarbons containing an aromatic ring; carbohydrates (Carb) are compounds consisting only of carbon (C), hydrogen (H), and oxygen (O); lignin-derived compounds (LgC) are organic compounds that feature aromatic ring(s), along with hydroxyl and ether groups; nitrogen-containing compounds (Ntg) refer to compounds that contain nitrogen (N); polyaromatic hydrocarbons (PAH) are hydrocarbons that contain more than one aromatic ring; phenolic compounds (PhC) are organic compounds with aromatic ring(s) and hydroxyl groups; saturated hydrocarbons (SaH) are compounds made up of only C and H atoms that satisfy Equation 1; and unsaturated hydrocarbons (UnSaH) are compounds composed solely of C and H, which do not fit the SaH equation (Equation 1). The compound list and the respective compound groups are shown in Supplementary Table S1.

$$C \times 2 + 2 = H + (number\ of\ rings \times 2) \quad (1)$$

2.2.3 Fluorescence spectroscopy

The composition of DOM of the biweekly sampled soil water was characterized by ultraviolet and visible light (UV–Vis) absorbance and excitation–emission matrix (EEM) fluorescence spectroscopy using the HORIBA AquaLog (HORIBA Scientific, Kyoto, Japan). The scanning fluorometer was vertically mounted with a 150 W xenon arc lamp. The analysis was performed employing excitation intensity of 240–600 nm with an increment of 2 nm (Broder et al., 2017) and the emission intensity was measured between 250.07 and 831.36 nm with an increment of 1.16 nm (2 pixels). To minimize the reduction in fluorescence intensity by the internal filter effect, samples with DOC concentrations greater than 9.50 mg L^{-1} were diluted with deionized water until the absorption at 254 nm was less than 0.3 units (Ohno, 2002). Dilution ratios were chosen according to DOC concentrations and ranged from 2 to 50 (Ohno, 2002; Kothawala et al., 2012). Deionized water was used for blank correction as well as for EEMs normalization using the Raman peak at 397 nm (350 nm excitation).

The UV absorbance at 254 nm (UVA254), fluorescence index (FI), and fluorescence peaks were obtained using the staRdom package in R version 4.4.1 (R Core Team, 2024), applying the methodology of Pucher et al. (2019) and related to the origin of DOM or DOM characteristic, i.e., aromaticity. According to Coble (1996), Parlanti et al. (2000), Hudson et al. (2007) and Fellman et al. (2010), specific fluorescence peaks were identified and analyzed according to their emission/excitation wavelengths in nm (Ex/Em), which reflect their biogeochemical nature. Humic-like peaks A (260/380–460, Ex/Em) and C (350/420–480, Ex/Em) represent DOM primarily derived from vascular plant sources, characterized by aromatic structures, high conjugation, and higher molecular weights. Peak M (312/380–420, Ex/Em), another humic-like component with emission at shorter wavelengths, indicates DOM of lower aromaticity and molecular weight, associated with both aquatic production and terrestrial inputs. Protein-like fluorophores were identified as peak B or tyrosine-like peak (275/310, Ex/Em) and peak T or tryptophan-like peak (275/340, Ex/Em), which represent mixtures of amino acids and similar fluorescing compounds rather than pure amino acids. These protein-like components served as indicators of DOM lability and microbial-derived organic matter. The relative intensities of the peaks were used to differentiate between terrigenous and autochthonous DOM sources in the samples.

The fluorescence index (FI) was calculated as the ratio of emission intensities at 450 nm and 500 nm (excitation at 370 nm) (McKnight et al., 2001). It serves as indicator of DOM source, with higher values (approximately 1.8) suggesting microbial and algal origins (Xu et al., 2023; Liu et al., 2020; Fenner and Freeman, 2011), while lower values (approximately 1.2) indicate terrestrially derived DOM from plant and soil organic matter (Fellman et al., 2010; McKnight et al., 2001; Cory and McKnight, 2005). The specific UV absorbance at 254 nm (SUVA254), was obtained by dividing the UV absorbance at 254 nm by the respective DOC concentration of the samples.

2.3 Statistical analysis

Bray-Curtis dissimilarity analysis was applied to datasets from the automated pipeline of the Py-GC/MS results, incorporating both individual compounds and compound groups, as well as absorbance and fluorescence indices/peaks. The main purpose of this analysis was to quantify the similarity across the different soils and along the depth gradient based on the obtained pyrolysates and compound groups (Py-GC/MS) and on the optical properties. This analysis was conducted using the vegdist function from the vegan package (Oksanen et al., 2020) in R version 4.4.1 (R Core Team, 2024). Similarity tables were derived by converting dissimilarity values to similarity percentages, which was accomplished by subtracting the dissimilarity value from 1, then multiplying the result by 100.

Principal component analysis (PCA) was conducted on the individual identified pyrolysates, compound groups, and optical parameters. The PCA explains the variance of the data with the principal components (PC). A higher explained variance indicates that a PC better represents the total variance in the dataset. The PCA was performed using RStudio Desktop version 4.2.2, with the analysis carried out using the FactoMineR (Lê et al., 2008) package and visualizations generated with factoextra (Kassambara and Mundt, 2020).

3 Results

3.1 DOM characterization

According to Table 2, the chemical and optical properties as well as DOM composition based on molecular markers from pyrolysates

TABLE 2 Dissolved organic matter characterization: 1) DOC and DON concentrations, DOC:DON ratio; 2) relative intensity of the absorbance and fluorescence indices, where SUVA254 = specific absorbance at 254 nm, FI = fluorescence index, B = tyrosin-like peak, T = tryphtophan-like peak, A = humic-like peak (recent material), M = microbial by-product peak, C = humic-like peak; 3) Py-GC/MS identified data as a percentage of compound group found in the soil water samples of different soils (Peat, peaty Gleysol, Cambisol, Podzol) at different depths (D1 = depth 1; D2 = depth 2; and D3 = depth 3). ArH = aromatic hydrocarbons, Carb = carbohydrates, LgC = lignin-derived compounds, Ntg = nitrogen containing compounds, PAH = Polyaromatic hydrocarbons, PhC = phenolic hydrocarbons, SaH = saturated hydrocarbons, UnSaH = unsaturated hydrocarbons, Uid = unidentified (i.e., unknown origin).

Sample	C and N parameters			Absorbance index	Fluorescence indices/ peaks						Py-GC/MS – Compound group (%)								
	DOC (mg L^{-1})	DON (mg L^{-1})	DOC: DON	$SUVA_{254}$ ($L.mg^{-1}$ m^{-1})	FI	B	T	A	M	C	ArH	Carb	LgC	Ntg	PAH	PhC	SaH	UnSaH	Uid
Peat D1	53.9 ± 29.0	1.9 ± 1.1	34.8 ± 7.4	5.7	1	0.1	0.3	3.7	2.3	3	7.9	18.8	4.8	33.7	0.2	22.1	1.0	1.5	10.0
Peat D2	44.3 ± 3.0	1.4 ± 0.6	35.4 ± 8.9	5.2	1.2	0.5	0.7	5.4	3.9	4.2	12.4	28.5	1.0	3.2	1.9	31.3	5.0	3.5	13.2
Peat D3	42.3 ± 2.1	1.2 ± 0.6	38.8 ± 9.1	4.3	1.1	0.6	0.8	5.1	3.8	4.1	10.9	27.9	1.3	4.3	1.7	35.2	1.3	3.2	14.2
Peaty Gleysol D1	37.6 ± 10.9	1.4 ± 1.2	30.8 ± 7.6	5.0	1.2	0.1	0.3	4.3	2.5	3.1	16.1	16.7	0.7	45.5	0.8	10.4	2.5	1.5	5.8
Peaty Gleysol D2	14.3 ± 2.7	0.6 ± 0.2	25.7 ± 6.2	4.6	1.2	0.1	0.2	2.5	1.5	1.8	14.5	11.4	0.0	6.6	1.8	11.9	43.4	3.7	6.7
Peaty Gleysol D3	14.0 ± 5.3	0.6 ± 0.3	23.4 ± 5.7	4.1	1.2	0.1	0.2	2.2	1.4	1.6	16.3	22.6	0.0	13.9	3.5	17.5	5.1	10.1	11.0
Cambisol D1	75.4 ± 40.2	3.5 ± 2.4	22.4 ± 5.2	5.0	1.1	0.2	0.7	7.8	5.2	5.4	14.5	25.0	8.3	28.1	2.2	9.2	5.7	1.7	5.3
Cambisol D2	5.8 ± 5.8	0.5 ± 0.1	12.3 ± 8.4	2.4	1.5	*	0.1	0.5	0.4	0.4	11.8	27.4	0.0	20.8	3.7	4.3	19.4	2.9	9.7
Cambisol D3	3.4 ± 1.8	0.5 ± 0.3	7.7 ± 2.6	1.6	1.6	*	0.1	0.5	0.3	0.3	6.8	44.8	0.0	27.2	0.9	0.5	1.5	15.3	3.0
Podzol D1	124.1 ± 89.7	7.2 ± 9.9	23.4 ± 7.0	5.3	1.0	0.3	1.0	12.3	7.8	9.2	21.6	26.0	3.6	24.9	1.1	7.4	2.4	4.6	8.4
Podzol D2	58.2 ± 13.1	2.1 ± 0.7	29.3 ± 6.1	4.7	1.2	0.2	0.7	8.0	5.0	5.9	30.7	25.8	0.0	10.8	3.2	8.3	8.3	5.1	7.8
Podzol D3	16.0 ± 3.0	0.8 ± 0.3	21.5 ± 5.2	3.4	1.4	0.1	0.3	2.8	1.8	2.2	31.7	24.1	0.0	13.8	7.9	7.8	1.9	5.7	7.1

10.3389/fenvs.2025.1675720

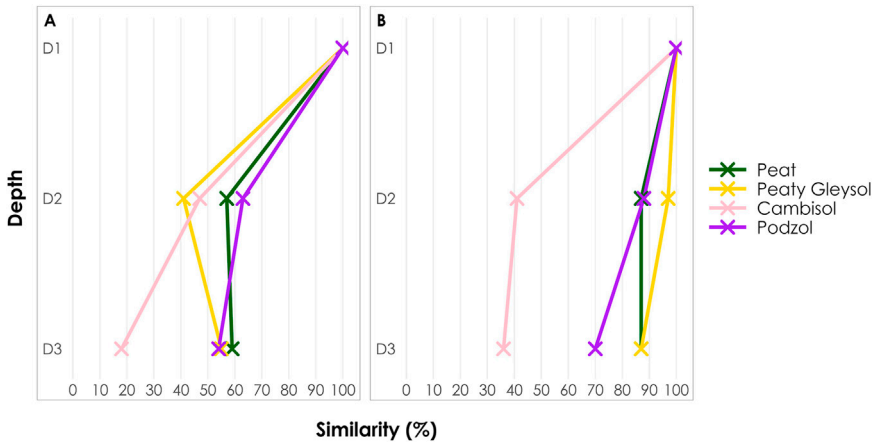

FIGURE 2
Changes in pair-wise similarity, according to the Bray-Curtis dissimilarity analysis, in percentage of DOM composition along soil profiles (Peat, peaty Gleysol, Cambisol, Podzol) considering the relative abundance of the identified chemical compounds derived from Py GC/MS **(A)** and optical indices from absorbance and fluorescence **(B)**. Depth 1 = D1, depth 2 = D2 and depth 3 = D3.

(hearafter referred to as "DOM composition") varied across soil types and depths. DOC and DON concentrations were highest in organic horizons at all sites, with greater variability in the forest floor of the Cambisol and the Podzol. This was evidenced by the standard deviations.

In the Peat, the smallest decrease in DOC and DON concentrations with soil depth ocurred, while DOC:DON ratios increased. $SUVA_{254}$ values decreased, with the FI remaining roughly at 1.1 indicating terrestrial origin. Fluorescence peaks B, T, A, M, and C, as well as phenolic compounds (22.1%–35.2%) increased with depth, while N compounds decreased considerably. Aromatic hydrocarbons and carbohydrates increased down to the second depth (12.4% and 28.5%, respectively), with a small decrease at D3. Lignin compounds were found at all depths of the Peat, decreasing from the first to the second sampling depth (D2) but without any further change down to the third sampling depth (D3).

In the peaty Gleysol, the DOC and DON concentrations decreased strongly at D2 (Table 2), with a decrease observed in the DOC:DON ratio. Also, the SUVA254 decreased from the first to the third sampling depth (D1 to D3). The FI remained constant and within a range typical for terrestrially-derived components. While the B index remained stable at 0.1, other fluorescence indices (T, A, M, and C) showed decreasing trends with depth. The decrease from D1 to D2 was much sharper than from D2 to D3, probably due to the change from an organic to a mineral soil horizon. A strong increase was observed in saturated hydrocarbons at D2, accompanied by fluctuations in carbohydrate content along the different depths. The distribution of compound groups showed similarities with the patterns of Peat DOM composition, particularly in the patterns of aromatic hydrocarbons and phenolic compounds.

The Cambisol displayed the strongest decrease in DOC and DON concentrations and in DOC:DON ratios with depth from D1 to D3 (Table 2). $SUVA_{254}$ showed also a sharp decrease while FI increased, indicating microbial DOM sources. Fluorescence peaks decreased sharply, especially peak A. Carbohydrates content increased consistently with depth, while lignin compounds were not detected in deeper layers using the Py-GC/MS approach. While there were some initial similarities in SUVA254 values at D1, the Cambisol showed distinctly different patterns in both optical properties and compound group distributions compared to both the organic Peat and the organic-rich peaty Gleysol.

The Podzol showed a steady decrease of DOC concentrations with depth and the highest DON variability at D1 (Table 2), with consistent decrease of concentration with depth. The variability in DOC:DON ratios of the Podzol was highest at D1 and showed a decreasing trend along the sampling depths. The $SUVA_{254}$ value decreased, the FI increased, and all fluorescence peaks decreased with depth, particularly peak A (12.3–2.8). Regarding the molecular composition, aromatic and polyaromatic hydrocarbons increased with depth, contrasting with the Cambisol patterns, while carbohydrate content showed a slight decrease. Phenols did not change with depth, but saturated hydrocarbons showed the highest enrichment in D2 (8.3%).

3.2 Similarity

3.2.1 Similarity along the depth gradient for the different soil types

To quantify the extent of DOM transformation with depth along the different soil types, two analytical approaches were used to evaluate the pair-wise similarity (i.e., Bray-Curtis dissimilarity analysis) between the DOM from the uppermost sampling depth (i.e., D1) with the deeper ones (i.e., D2 or D3). The first approach was using the data from the Py-GC/MS analysis, which included the relative abundance of the identified chemical compounds (Figure 2A). The second approach was the use of the optical parameters from the fluorescence spectroscopy data (Figure 2B).

Py-GC/MS compositional similarity generally decreased with depth across the sites (Figure 2A), while spectroscopic indices did not reflect this trend (Figure 2B). In the Peat, DOM revealed moderate compositional changes (57%–59% similarity of

TABLE 3 Changes in similarity (%) of dissolved organic matter composition in soils (Peat, peaty Gleysol, Cambisol, Podzol) with depth (D1, D2, D3) according to pyrolysis-gas chromatography/mass spectroscopy (Py-GC/MS; i.e., relative abundance of the identified chemical compounds) and optical properties data (absorbance and fluorescence indices/peaks).

Sample	Py-GC/MS			Optical properties		
	Similarity (%) to the peat			Similarity (%) to the peat		
	D1	D2	D3	D1	D2	D3
Peaty Gleysol	66%	42%	55%	92%	93%	88%
Cambisol	49%	33%	11%	91%	45%	39%
Podzol	48%	40%	29%	89%	95%	87%
	Similarity (%) to the peaty Gleysol			Similarity (%) to the peaty Gleysol		
	D1	D2	D3	D1	D2	D3
Cambisol	55%	36%	12%	93%	47%	47%
Podzol	54%	37%	45%	87%	90%	80%
	Similarity (%) to the Cambisol			Similarity (%) to the Cambisol		
	D1	D2	D3	D1	D2	D3
Podzol	57%	33%	12%	93%	45%	33%

chemical compounds) with depth, with invariable spectroscopic characteristics (approximately 90%). DOM in the peaty Gleysol showed a sharp drop in the similarity of chemical compounds from the first to the second sampling depth (from 100% to 41%; Figure 2A), followed by an increase in similarity down to the third sampling depth (D3; 55%). The DOM in the Cambisol underwent the most intensive compositional changes with depth, reaching the lowest similarities at D3 among all sites (18% for the chemical compounds, and 36% fluorescence spectroscopy). The DOM in the Podzol displayed intermediate compositional patterns, with progressive decreases in both chemical (54% at D3) and spectroscopic (54% at D3) similarities with depth.

For Peat, peaty Gleysol, and Podzol, the moderate chemical (54%–59%; Figure 2A) and higher spectroscopic similarity (70%–87%; Figure 2B) of DOM in the deeper subsoils suggest that some characteristics of the DOM from the organic horizons persisted in deep subsoils. In contrast, the low similarity values found in Cambisol D3 suggested that intensive soil processes can transform DOM signatures to such an extent that the original input driven by vegetation and its litter no longer shapes deep subsoil DOM composition.

3.2.2 Similarity across different sites

The similarity across different soil types at corresponding depth positions was also assessed by similarity analysis, and the results are summarized in Table 3.

The similarity analyses revealed distinct patterns in DOM composition across sites, with again higher similarities for optical properties compared to Py-GC/MS data, i.e., relative abundance of the identified chemical compounds (Table 3). This divergence reflects fundamental analytical differences. Different compounds sharing similar chromophoric structures obviously yield comparable fluorescence signals despite distinct molecular identities (Stedmon and Bro, 2008). For example, phenolic compounds having different side chains and functional groups can yield similar fluorescence signatures (Cory and McKnight, 2005). Given that Py-GC/MS provided greater specificity in detecting compositional differences at the molecular level (Figure 2; Table 3), subsequent analyses will focus mainly on Py-GC/MS data.

Similarities of the optical properties (Table 3) remained fairly high for most of the pair-wise comparison among the different soil types (80%–93%). The lowest similarities were observed with the Cambisol at D2 and D3 (Peat-Cambisol: 45% and 39%, respectively; peaty Gleysol-Cambisol: 47% and 37%, respectively; and Podzol-Cambisol: 45% and 33%, respectively).

In regard to the Py-GC/MS data similarities, at D1, DOM composition was moderately similar (48%–66%, Py-GC/MS) at all sites. The Peat and the peaty Gleysol DOM shared the highest similarity (66%). Peat DOM composition was less similar to DOM from sites with forest floors (Cambisol and Podzol, both <50%), while the Cambisol and the Podzol DOM composition were moderately similar (57%). With increasing depth, similarities decreased even more across all sites. At D2, similarity was in the range of 33%–42% (Table 3), with Peat DOM composition being most similar to DOM of the peaty Gleysol (42%) and the Podzol (40%). Peaty Gleysol DOM was more similar to DOM of the Cambisol (36%) and the Podzol (37%) than the similarity of DOM composition between these two mineral sites (33%). The lowest similarities occurred at the deepest sampling positions. It was 11% for the Peat-Cambisol comparison, 12% for both peaty Gleysol-Cambisol and Cambisol-Podzol DOM comparisons, indicating the Cambisol to have the most unique DOM composition across deeper subsoils. Moderate similarity of deep subsoil DOM composition was found for the Peat and peaty Gleysol (55%), probably reflecting the influence of DOM from their organic forest floors. The moderate similarity of DOM composition of the peaty Gleysol and the Podzol (45%) suggests mineral subsoil influences in the peaty Gleysol profile. These decreasing similarities with depth reflect the increasing influence of site-specific pedogenic processes.

4 Discussion

4.1 Processes shaping the DOM composition along soil profiles

In the Peat, the observed changes in DOM composition were consistent with the preservation of many plant-derived compounds under anoxic conditions. Minimal variability of the number of identified Py-GC/MS compounds, i.e., compound number (n = 53–54; Supplementary Figure S1), in combination with relatively small decreases in DOC and DON concentrations with depth (Supplementary Table S2), suggested limited changes in DOM composition. The moderate to high compositional similarity observed along the profile (Figure 2) supports the assumption that DOM composition remained fairly unaltered, possibly allowing the compositional signatures from D1 to remain in deeper horizons, D3 (59% of similarity; Figure 2A). Suppressed decomposition under anoxic conditions and presumably the limited importance of sorptive alteration were possibly the causes to the lack of major DOM composition changes along the depth gradient. Constantly high SUVA254 and low FI (Table 2) indicated terrestrially-derived DOM (D'Andrilli et al., 2022; Cory et al., 2010; McKnight et al., 2001). The high humic-like (A, M, C) and stable protein-like fluorescence peaks (B, T), Table 2, suggested little microbial processing under sustained anoxic conditions (Huguet et al., 2009; Coble, 1996). Though the apparent persistence of key phenolic compounds such as p-cresol and phenols (PhC 7, 3, and 5, respectively; Supplementary Figure S2) is typical for anoxic conditions, as limited oxygen availability inhibits oxidative enzymes (Bourdon et al., 2023; Wang et al., 2015; Freeman, 2011), they could also arise from the continuous breakdown of larger macromolecules.

The Cambisol showed the strongest changes in DOM composition with depth, with not only the highest number of compounds at D1 (n = 63; Supplementary Figure S1), but also strong changes in optical features (Table 2) and in similarities (Figure 2). DOM composition similarities between D1 and D3 was approximately 18% (Figure 2A), suggesting that the deeper mineral subsoil reflected poorly the DOM composition from the overlying organic horizon. Plant-derived phenolics progressively decreased evidenced by the depletion of respective plant markers (furfural, Carb 24; Supplementary Figure S3), while carbohydrates increased (Table 2) mainly due to an enrichment of microbial metabolites (e.g., 5-Hexenoic acid, Carb 6; Supplementary Figure S3). This suggests that DOM composition is potentially microbially-derived (Roth et al., 2019), either due to increased alteration from microbial processing and/or contribution of microbial necromass (Finley et al., 2025), or as a result of preferential sorption of plant-derived compounds to the soil mineral phases according to Kaiser and Kalbitz (2012). The decrease of humic-like fluorescence peaks (Table 2), DOC and DON concentrations and DOC:DON ratios (Supplementary Table S2) could be similarly linked to both microbial processing or/and preferential sorption (Groeneveld et al., 2023; Kramer et al., 2012; Kaiser et al., 2002; Cory and McKnight, 2005; McKnight et al., 2001). However, the strong decrease in aromatic hydrocarbons (from 15% to 6.8%; Table 2) could be indicative of efficient sorptive retention (Moni et al., 2010) rather than decomposition (Leinemann et al., 2018).

In the Podzol, the decreasing identified compound numbers (n = 57 to n = 47; Supplementary Figure S1) combined with the gradual decrease in compositional similarity (54%; Figure 2B) first indicated that although DOM composition may have changed, signals from the organic layer still can be traced in deep mineral subsoil. The increased DOC:DON ratio at the uppermost mineral subsoil (D2) pointed toward microbial uptake and selective retention of organic N, as proteins can sorb strongly to minerals by the combination of electrostatic forces and hydrophobic interactions (Kleber et al., 2007). The reduction in fluorescence peaks T and B (Table 2) also supports the idea of a possibly strong retention of protein-type compounds. While DOM composition underwent substantial changes with depth in both the Cambisol and the Podzol, the main mechanisms promoting the changes differed between the two soils. The higher pH (6.4 ± 1.1; Supplementary Table S3) in the Cambisol potentially created more favorable conditions for microbial activity (Kaiser and Kalbitz, 2012), while low pH conditions (4.3 ± 0.2; Supplementary Table S3) in the Podzol most likely resulted in the formation of soluble organo-metal complexes. These complexes are mobile and were likely transported downward during podzolization (Ferro-Vázquez et al., 2014; Bogner et al., 2012). Therefore, formation of soluble organo-metal complexes and their re-precipitation was potentially the main process that led to changes in DOM composition. This also coincides with the gradual decrease in compositional similarity (Supplementary Table S4) and DOC concentrations (Supplementary Table S2) found in the Podzol when compared to the Cambisol.

In the peaty Gleysol, the change in DOM composition between the two upper sampling depths was pronounced, with N compounds decreasing strongly and saturated hydrocarbons increasing considerably (Table 2). This shift, along with the increased number of Py-GC/MS identified compounds (n = 53 to n = 60; Supplementary Figure S1), and the accumulation of long-chain saturated hydrocarbons (SaH 3–11; Supplementary Figure S4), suggested selective preservation of such compounds under frequent changes in oxic and anoxic conditions (Fellman et al., 2010; Jansen and Nierop, 2009; Cory and McKnight, 2005). Despite lower similarity between D1 and D2 (41%; Supplementary Table S4) than between D1 and D3 (55%; Supplementary Table S4), the spectroscopic similarity remained high (87%–97%; Supplementary Table S5). This suggests that the DOM composition may change by selective degradation and sorption, as identified using the Py-GC/MS approach, but still retain moieties contributing to rather similar fluorescence signals (Tfaily et al., 2013). The 55% of DOM composition similarity between D1 and D3 according to the Py-GC/MS was considered to be moderate, highlighting that signals from the overlying organic horizon may be detected in deeper mineral subsoil. Contrasting the Peat, the increase in carbohydrate content of DOM with depth in the peaty Gleysol (Table 2) suggested active but moderate microbial processing, i.e., presence of furan derivatives (Huber et al., 2010), cyclic compounds (Perry and Gibson, 1977), and methyl formate (Gunina and Kuzyakov, 2015; Schulten and Schnitzer, 1997). This was observed through the preservation of simple sugars as well as formation of cyclic structures (Carb 27–30; Supplementary Figure S3). These patterns, along with the moderate decrease in

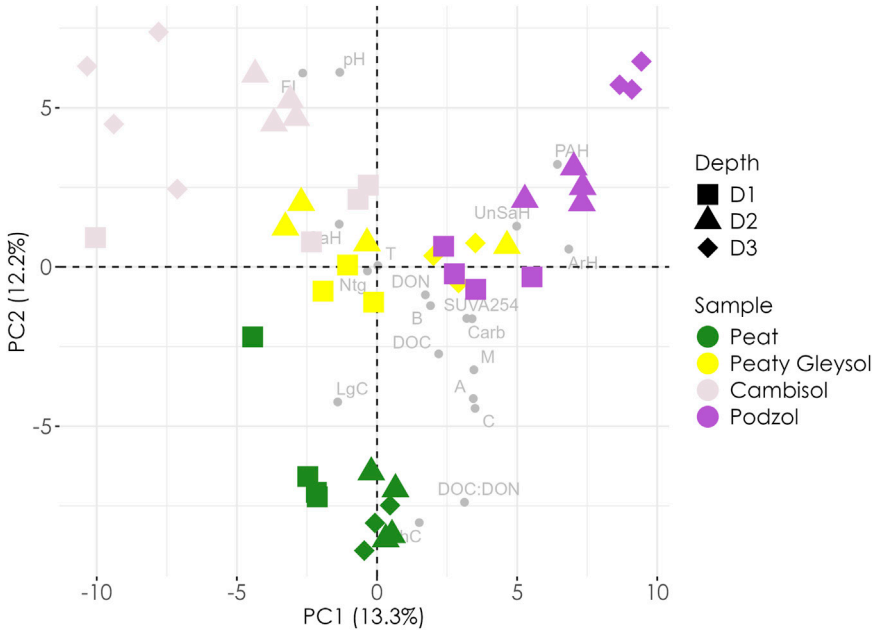

FIGURE 3
Results of the principal component analysis (PCA) of the parameters analyzed (dots in gray color) in this study for all the sites (Peat, peaty Gleysol, Cambisol and Podzol) at depth 1, 2 and 3 (D1, D2 and D3, respectively). FI = fluorescence index, B = tyrosin-like peak, T = tryphtophan-like peak, A = humic-like peak (recent material), M = microbial by-product peak, C = humic-like peak, SUVA254 = absorbance at 254 nm, ArH = aromatic hydrocarbon, Carb = carbohydrate, LgC = lignin compound, Ntg = nitrogen containing compound, PAH = Polyaromatic hydrocarbon, PhC = phenolic compound, SaH = saturated hydrocarbon, UnSaH = unsaturated hydrocarbon. The PCA also considered the relative abundance of all the chemical compounds, however, it is not shown in the figure to improve its readability.

similarity of peaty Gleysol between D1 and D2 (Supplementary Table S4), indicate that depth-related changes in DOM composition in the peaty Gleysol reflect processing intermediate between that in organic (i.e., preservation under anoxia, less sorption) and mineral soils (i.e., microbial processing and sorption). However, based on Py-GC/MS and optical properties alone, it was not possible to identify which process was the main driver.

Overall, DOM compositional similarity in the Peat decreased less strongly, possibly enabling to trace DOM composition along the depth gradient. We attribute the moderate changes in compositional similarities to the anoxic conditions present in the soil. In contrast, the substantial changes of DOM composition observed in the Cambisol suggested strong sorptive retention combined with some microbial degradation, resulting in minimal potential to trace DOM composition from the forest floor to the deeper mineral subsoil. The Podzol and the peaty Gleysol showed more moderate changes in DOM composition, presumably driven by a combination of biotic and abiotic processes. Although not measured in this study, microbial and fungal necromass may represent an important source of stabilized organic matter. Its analysis in future work could help link the observed changes in DOM composition with long-term carbon persistence, as microbial residues are chemically suited for sorption to minerals, promoting carbon stabilization in deeper layers (Liu et al., 2023; Tian et al., 2021). In sum, these results suggested that similarity of DOM composition decreased with depth within all the individual soil profiles, though DOM from overlying organic horizon may still be identified in deeper soil horizons depending on the soil processes. These findings reflect the importance of the different in-soil processes and thereby supporting the first hypothesis and partially the second.

4.2 Towards a uniform DOM composition with depth?

The central question of whether DOM compositions are becoming more similar with soil depth across the soil types was first tested with a multivariate analysis (Figure 3).

The PCA analysis shown in Figure 3 revealed distinct DOM composition for each soil type, which not only persisted but even became more pronounced with depth. This contradicts the hypothesis of increasing similarity across the different soil types with depth. The loadings on the components may be interpreted as relative influence of individual ongoing soil processes. The first principal component (PC1) apparently captured differences in transformation mechanisms, which ultimately differentiate the DOM composition across the soils and with depth. The second component (PC2) was associated with aromaticity indicators (e.g., $SUVA_{254}$, humic-like peaks A, M, and C) and DOC concentration, separating the Peat profile from the sites with mineral subsoils. This was particularly evident in the negative loadings of phenolic compounds and DOC:DON ratio on PC2, as the Peat DOM composition was indeed characterized by high phenolic contents and high DOC:DON ratios (Table 2). Instead, FI and aromatic hydrocarbon contents, for which high values were observed for the Cambisol, peaty Gleysol and the Podzol, had positive loadings. At D1, topsoil samples clustered closely around the centroid in the

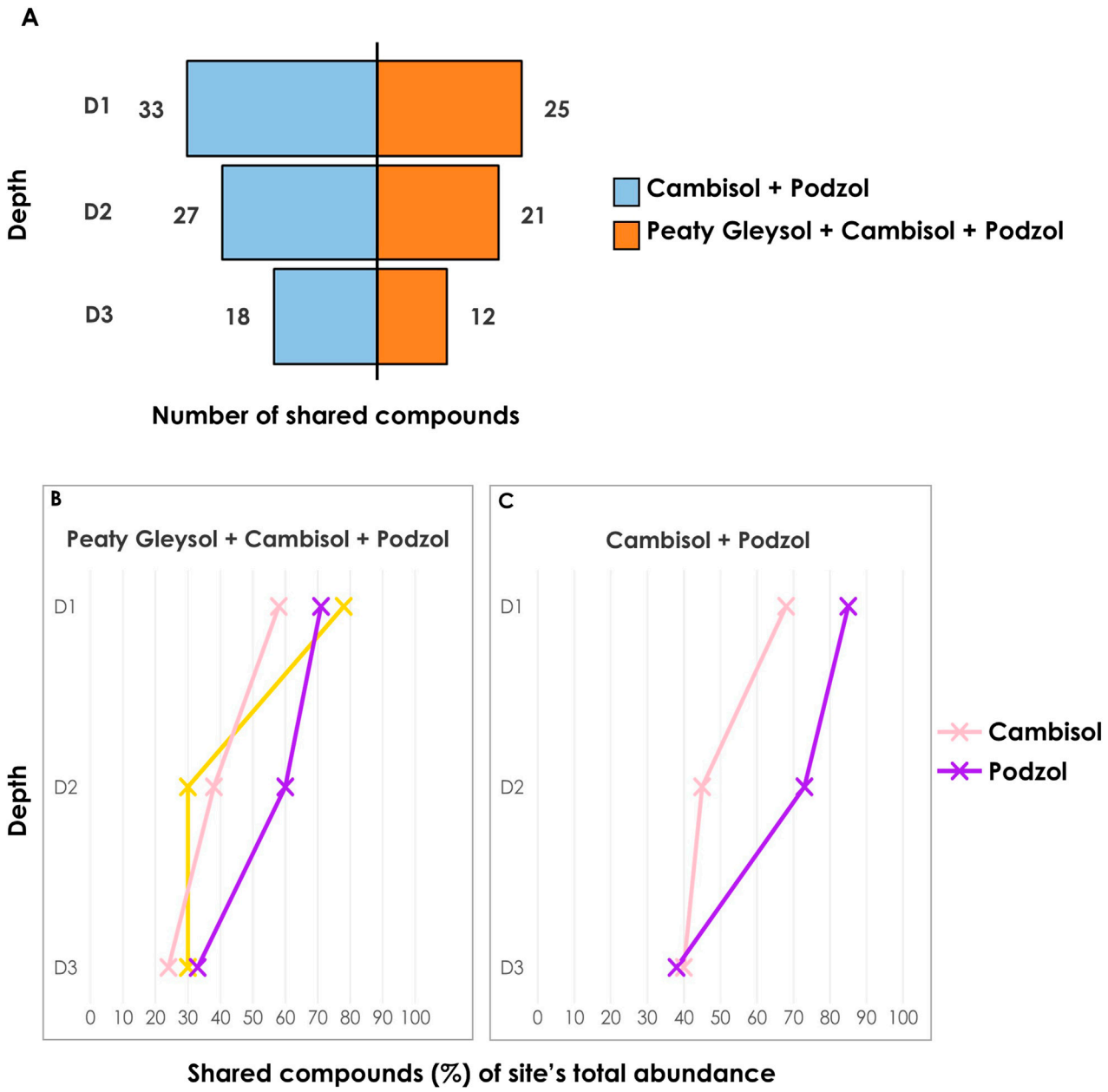

FIGURE 4
(A) Bar chart of the numbers of shared individual compounds in dissolved organic matter (DOM) samples of soils with mineral subsoils (Cambisol and Podzol, represented by blue color) and peaty Gleysol, Cambisol, and Podzol, represented by orange color, at different depths. The line plots represent the contribution (%) of shared compounds to total DOM in each soil at each depth using two approaches **(B)** mineral soils (i.e., Cambisol and Podzol) and **(C)** all soils that contain mineral subsoils (i.e., peaty Gleysol, Cambisol, Podzol). D1 = depth 1, D2 = depth 2, D3 = depth 3.

PCA, indicating relatively similar DOM composition across sites. With increasing depth, however, the samples became progressively more dispersed, moving in divergent directions in the PCA. By depth 3, all investigated soils were rather dissimilar and had distinct molecular signatures.

To further investigate the potential reasons for the dissimilarity in DOM composition across the sites at comparable depths, we examined the number of shared compounds based on the Py-GC/MS analysis and their relative contribution (Figure 4). The analysis shown in Figure 4 excluded Peat as apparently the distinct conditions under anoxia caused a preservation of DOM composition irrespective of depth. Thus, for further comparison across profiles, the sites that undergone active transformation through microbial processing, mineral adsorption, and/or organo-metal complexation were used with two comparison strategies. The first comparison of similarities was done with the two soils featuring mineral horizons throughout their profiles (Cambisol and Podzol). The second comparison was performed including the peaty Gleysol and the mineral soils to examine whether any soil containing mineral horizons at depth develops a

similar DOM composition regardless of the surface horizon properties.

In the organic topsoil horizons (D1; Figure 4A), DOM composition showed substantial overlap between sites with mineral subsoil. Mineral soils shared 33 compounds (Cambisol and Podzol; blue bars), which represented more than half of the total number of individual compounds identified in each soil (n = 63 for the Cambisol, n = 57 for the Podzol; Supplementary Figure S1). This compositional overlap was reflected by the moderate similarities between sites at D1 (48%–66%; Table 3), with forest floor sites showing 57% similarity. When including the peaty Gleysol, shared compounds decreased to 25 (orange bars; Figure 4A). With depth, shared compounds continued to decrease despite increases in total compound numbers in some soils (peaty Gleysol: n = 53 to n = 60 at D2; Cambisol: n = 63 to n = 67 at D2; Supplementary Figure S1). By D3, shared compounds represented only 38% of total compounds in the Cambisol and Podzol (both with n = 47; Figure 4A; Supplementary Figure S1), and this percentage decreased again to 25% when including the peaty Gleysol (orange bars; Figure 4A; Supplementary Figure S1). This depth-related decline in similarity was consistent with patterns observed in hydrophilic compounds found in the soil organic matter, where decomposition processes similarly decreased molecular diversity and ecosystem similarity with depth (Davenport et al., 2023). However, the number of shared compounds alone provides incomplete information, as fewer shared compounds might still dominate absolute DOM composition if highly abundant.

To address whether the shared compounds dominate the overall composition of the DOM, Figures 4B,C show the relative abundance of shared compounds. For the Cambisol and Podzol (Figure 4B), the shared compounds at D1 constituted 68% and 84% of the total compound abundances, respectively, but this contribution decreased to around 40% for both sites at D3. This demonstrated that both the number and the relative contribution of shared compounds declined with depth, confirming the increasing degree of dissimilarity among the investigated soils. Interestingly, when analyzing all three sites with mineral subsoils (peaty Gleysol, Cambisol, Podzol; Figure 4C), shared compounds represented an even smaller proportion of total DOM at D1 (58%–78%) as compared to the Cambisol and Podzol alone. Their contribution decreased even more with depth, being as low as 25% in the Cambisol at D3. The cross-soil similarity analysis (Table 3) corroborated this divergence, showing that similarities between soils decrease substantially with depth, with the Cambisol becoming the most distinct (11%–12% similarity with all soils at D3), while the Peat and peaty Gleysol maintained moderate similarity (55%). This was likely due to limited decomposition under (temporary) anoxia and potentially due to more contribution of sorption in the mineral soils compared to the organic soils (Li et al., 2022; Kothawala et al., 2009). Analysis of soil profiles revealed that the decrease in shared compounds and their relative abundance with depth resulted in distinct DOM signatures for each soil type rather than having a similar DOM composition, as proposed by Freeman et al. (2024), due to different in-soil processes. This soil-type specific differentiation also aligns with recent findings that soil organic matter molecular diversity patterns depend on ecosystem type, with different mechanisms operating in different soils (Tian et al., 2025). Despite the transformations and decreasing similarities, the organic horizon characteristics remained traceable in deeper layers across all sites except of the Cambisol. According to the similarity analysis (Figure 2), this persistence of organic signatures in subsoil DOM has significant implications. Firstly, DOM composition is partially governed by vegetation inputs and organic horizon characteristics, creating site-specific molecular fingerprints that persist through the soil profile. Secondly, these distinct signatures may enable source tracking when soil water reaches streams through lateral flow via groundwater (i.e., base flow conditions), and under high flow conditions, with water mostly passing only surface-near soil compartments before entering the surface waters. The transfer of site-specific DOM fingerprints into streams influences not only the chemical diversity of stream water DOM but also its reactivity, persistence, and this ecological role in aquatic ecosystems. However, our findings are subjected to some limitations. Our analysis was constrained to a small number of soil types from one geographic region and climate. Broader studies encompassing different locations, climates, and soil types are needed to further prove our findings that DOM composition similarities decrease with depth. Additionally, pyrolysates are ultimately thermal decomposition products rather than intact, original DOM molecules (Dong et al., 2025), which may not fully capture the original DOM compositional diversity and could influence the observed patterns (Kaal et al., 2017). Therefore, it would be beneficial to apply other approaches, such as high-resolution mass spectrometry, to characterize DOM composition.

5 Summary and conclusion

This study shed new light on the complex and dynamic nature of DOM transformation in different soil profiles. Our analysis indicated that similarity of DOM as assessed by Py-GC/MS and optical properties decreased systematically with depth across all soil types, through different mechanisms. This compositional divergence was likely driven by site-specific processes: limited decomposition under anoxic conditions in the Peat, intense microbial processing and strong sorptive retention of stable plant-derived compounds in the Cambisol, microbial processing combined with the formation of organo-metal complexes in the Podzol, and selective preservation under anoxia, oxidative microbial processing and sorption in the peaty Gleysol. While the hypothesis of subsoil DOM retaining identifiable fingerprints from overlying organic layers was accepted, except for the Cambisol, the hypothesis of increasing similarity across the different soils at deeper horizons was strongly rejected. Mineral soils and soils containing mineral subsoils demonstrated remarkable decreases in both the number of shared compounds and their relative abundance at deeper horizons, indicating dissimilarity rather than similarity of DOM composition.

Our findings may be useful to understand how the compositional divergence could potentially impact the long-term C storage and predict the inputs and subsequent effects of DOM entering aquatic ecosystems from different soils. Soil type-specific DOM processing with depth results in distinct molecular fingerprints, making subsoil DOM signatures traceable into

groundwater and surface water under varying flow conditions. In conclusion, our study demonstrates that DOM composition in deeper soil layers was shaped by two main factors: 1) the specific processes that control and shape the DOM composition of the different soil types, and 2) the source of organic matter, such as litter or microbial products. The results of detailed molecular and spectroscopic analyses challenge the assumption that DOM from different soils will eventually achieve a uniform composition. Instead, they highlight the importance of accounting for soil-specific DOM processing when predicting DOM inputs, their origins, and their impacts on aquatic ecosystems. Furthermore, our findings suggest that DOM fingerprinting in aquatic systems, particularly using Py-GC/MS, offers a valuable opportunity to trace DOM compositions back to specific soil-derived sources within a catchment.

Data availability statement

The raw data supporting the conclusions of this article will be made available by the authors, without undue reservation.

Author contributions

LC: Conceptualization, Data curation, Formal Analysis, Methodology, Software, Investigation, Writing – original draft, Writing – review and editing. TH: Conceptualization, Supervision, Writing – review and editing. KlK: Conceptualization, Supervision, Writing – review and editing. K-HK: Writing – review and editing. TK: Methodology, Writing – review and editing. HC: Methodology, Writing – review and editing. PK: Writing – review and editing. JH: Conceptualization, Writing – review and editing. IM: Conceptualization, Writing – review and editing. KaK: Conceptualization, Funding acquisition, Project administration, Supervision, Writing – review and editing.

Funding

The author(s) declare that financial support was received for the research and/or publication of this article. This study is funded by the Deutsche Forschungsgemeinschaft (DFG project number 452252890) and the Saxon State Office for Environment, Agriculture and Geology (Ref: 1-0452/202/26). Jakub Hruška and Pavel Krám received support from the Czech Science Foundation under Project No. 21-22810J.

Acknowledgments

We are grateful to Manuela Unger, Gisela Ciesielsk, and Josephine Hillig for their help with the laboratory analyses and to Dr. Falk Hieke for the detailed soil survey in the catchment area. We would like to thank Stephan Krüger for all his efforts during the initial phase of this project.

Conflict of interest

The authors declare that the research was conducted in the absence of any commercial or financial relationships that could be construed as a potential conflict of interest.

Generative AI statement

The author(s) declare that no Generative AI was used in the creation of this manuscript.

Any alternative text (alt text) provided alongside figures in this article has been generated by Frontiers with the support of artificial intelligence and reasonable efforts have been made to ensure accuracy, including review by the authors wherever possible. If you identify any issues, please contact us.

Publisher's note

All claims expressed in this article are solely those of the authors and do not necessarily represent those of their affiliated organizations, or those of the publisher, the editors and the reviewers. Any product that may be evaluated in this article, or claim that may be made by its manufacturer, is not guaranteed or endorsed by the publisher.

Supplementary material

The Supplementary Material for this article can be found online at: https://www.frontiersin.org/articles/10.3389/fenvs.2025.1675720/full#supplementary-material

References

Bogner, C., Borken, W., and Huwe, B. (2012). Impact of preferential flow on soil chemistry of a podzol. *Geoderma* 175, 37–46. doi:10.1016/j.geoderma.2012.01.019

Bourdon, K., Fortin, J., Dessureault-Rompré, J., and Caron, J. (2023). Mitigating decomposition in agricultural peatlands: influence of copper and polyphenol on CNP dynamics and enzyme activities in two contrasting soils. *Geoderma* 439, 116694. doi:10.1016/j.geoderma.2023.116694

Broder, T., Knorr, K. H., and Biester, H. (2017). Changes in dissolved organic matter quality in a peatland and forest headwater stream as a function of seasonality and hydrologic conditions. *Hydrol. Earth Syst. Sci.* 21 (4), 2035–2051. doi:10.5194/hess-21-2035-2017

Cannavo, P., Dudal, Y., Boudenne, J. L., and Lafolie, F. (2004). Potential for fluorescence spectroscopy to assess the quality of soil water-extracted organic matter. *Soil Sci.* 169 (10), 688–696. doi:10.1097/01.ss.0000146021.69183.5d

Charamba, L. V., Houska, T., Kaiser, K., Knorr, K. H., Krüger, S., Krause, T., et al. (2024). Tracing sources of dissolved organic matter along the terrestrial-aquatic continuum in the Ore Mountains, Germany. *Sci. Total Environ.* 943, 173807. doi:10.1016/j.scitotenv.2024.173807

Chen, H., Blosser, G. D., Majidzadeh, H., Liu, X., Conner, W. H., and Chow, A. T. (2018). Integration of an automated identification-quantification pipeline and statistical techniques for pyrolysis GC/MS tracking of the molecular fingerprints of natural organic matter. *J. Anal. Appl. Pyrol.* 134, 371–380. doi:10.1016/j.jaap.2018.07.002

Coble, P. G. (1996). Characterization of marine and terrestrial DOM in seawater using excitation-emission matrix spectroscopy. *Mar. Chem.* 51 (4), 325–346. doi:10.1016/0304-4203(95)00062-3

Cory, R. M., and McKnight, D. M. (2005). Fluorescence spectroscopy reveals ubiquitous presence of oxidized and reduced quinones in dissolved organic matter. *Environ. Sci. Sci. Technol.* 39 (21), 8142–8149. doi:10.1021/es0506962

Cory, R. M., Miller, M. P., McKnight, D. M., Guerard, J. J., and Miller, P. L. (2010). Effect of instrument-specific response on the analysis of fulvic acid fluorescence spectra. *Limnol. Oceanogr. Methods* 8 (2), 67–78. doi:10.4319/lom.2010.8.0067

Davenport, R., Bowen, B. P., Lynch, L. M., Kosina, S. M., Shabtai, I., Northen, T. R., et al. (2023). Decomposition decreases molecular diversity and ecosystem similarity of soil organic matter. *Proc. Natl. Acad. Sci. U.S.A.* 120 (25), e2303335120. doi:10.1073/pnas.2303335120

De Troyer, I., Amery, F., Van Moorleghem, C., Smolders, E., and Merckx, R. (2011). Tracing the source and fate of dissolved organic matter in soil after incorporation of a ^{13}C labelled residue: a batch incubation study. *Soil Biol. biochem.* 43 (3), 513–519. doi:10.1016/j.soilbio.2010.11.016

Dong, C., Huang, Y. H., and Li, M. (2025). Bacterial community assembly and the composition of dissolved and bulk organic matter varied along the salinity gradient in the Yangtze river estuary sediments. *Environ. Earth Sci.* 84 (14), 399. doi:10.1007/s12665-025-12401-2

D'Andrilli, J., Silverman, V., Buckley, S., and Rosario-Ortiz, F. L. (2022). Inferring ecosystem function from dissolved organic matter optical properties: a critical review. *Environ. Sci. Technol.* 56 (16), 11146–11161. doi:10.1021/acs.est.2c04240

Fellman, J. B., Hood, E., and Spencer, R. G. (2010). Fluorescence spectroscopy opens new windows into dissolved organic matter dynamics in freshwater ecosystems: a review. *Limnol. Oceanogr.* 55 (6), 2452–2462. doi:10.4319/lo.2010.55.6.2452

Feng, X., Simpson, A. J., and Simpson, M. J. (2005). Chemical and mineralogical controls on humic acid sorption to clay mineral surfaces. *Org. Geochem.* 36 (11), 1553–1566. doi:10.1016/j.orggeochem.2005.06.008

Fenner, N., and Freeman, C. (2011). Drought-induced carbon loss in peatlands. *Nat. Geosci.* 4 (12), 895–900. doi:10.1038/ngeo1323

Ferro-Vázquez, C., Nóvoa-Muñoz, J. C., Costa-Casais, M., Klaminder, J., and Martínez-Cortizas, A. (2014). Metal and organic matter immobilization in temperate podzols: a high resolution study. *Geoderma* 217, 225–234. doi:10.1016/j.geoderma.2013.10.006

Finley, B. K., Enalls, B. C., de Raad, M., Al Said, M., Chen, M., Joyner, D. C., et al. (2025). Unraveling the influence of microbial necromass on subsurface microbiomes: metabolite utilization and community dynamics. *ISME Commun.* 5 (1), ycaf006. doi:10.1093/ismeco/ycaf006

Freeman, E. C., Emilson, E. J., Dittmar, T., Braga, L. P., Emilson, C. E., Goldhammer, T., et al. (2024). Universal microbial reworking of dissolved organic matter along environmental gradients. *Nat. Commun.* 15 (1), 187. doi:10.1038/s41467-023-44431-4

Gabor, R. S., Baker, A., McKnight, D. M., and Miller, M. P. (2014). "Fluorescence indices and their interpretation," in *Aquatic organic matter fluorescence. Cambridge environmental Chemistry Series*. Editors P. G. Coble, J. Lead, A. Baker, D. M. Reynolds, and R. G. M. Spencer (Cambridge: Cambridge University Press), 303–338. Chapter.

Groeneveld, M., Kothawala, D. N., and Tranvik, L. J. (2023). Seasonally variable interactions between dissolved organic matter and mineral particles in an agricultural river. *Aquat. Sci.* 85 (1), 2. doi:10.1007/s00027-022-00898-9

Gunina, A., and Kuzyakov, Y. (2015). Sugars in soil and sweets for microorganisms: review of origin, content, composition and fate. *Soil Biol. biochem.* 90, 87–100. doi:10.1016/j.soilbio.2015.07.021

Hua, H., Liu, M., Liu, C. Q., Lang, Y., Xue, H., Li, S., et al. (2023). Differences in the spectral characteristics of dissolved organic matter binding to Cu (II) in wetland soils with moisture gradients. *Sci. Total Environ.* 874, 162509. doi:10.1016/j.scitotenv.2023.162509

Huber, S. G., Wunderlich, S., Scholer, H. F., and Williams, J. (2010). Natural abiotic formation of furans in soil. *Environ. Sci. Technol.* 44 (15), 5799–5804. doi:10.1021/es100704g

Hudson, N., Baker, A., and Reynolds, D. (2007). Fluorescence analysis of dissolved organic matter in natural, waste and polluted waters—a review. *River Res. Appl.* 23 (6), 631–649. doi:10.1002/rra.1005

Huguet, A., Vacher, L., Relexans, S., Saubusse, S., Froidefond, J. M., and Parlanti, E. (2009). Properties of fluorescent dissolved organic matter in the Gironde Estuary. *Org. Geochem.* 40 (6), 706–719. doi:10.1016/j.orggeochem.2009.03.002

IUSS Working Group WRB (2022). *World Reference Base for Soil Resources. International soil classification system for naming soils and creating legends for soil maps*. 4th edition. Vienna, Austria: International Union of Soil Sciences IUSS.

Jansen, B., and Nierop, K. G. (2009). Methyl ketones in high altitude Ecuadorian Andosols confirm excellent conservation of plant-specific n-alkane patterns. *Org. Geochem.* 40 (1), 61–69. doi:10.1016/j.orggeochem.2008.09.006

Jiang, T., Kaal, J., Liang, J., Zhang, Y., Wei, S., Wang, D., et al. (2017). Composition of dissolved organic matter (DOM) from periodically submerged soils in the Three Gorges Reservoir areas as determined by elemental and optical analysis, infrared spectroscopy, pyrolysis-GC–MS and thermally assisted hydrolysis and methylation. *Sci. Total Environ.* 603, 461–471. doi:10.1016/j.scitotenv.2017.06.114

Kaal, J., Cortizas, A. M., and Biester, H. (2017). Downstream changes in molecular composition of DOM along a headwater stream in the Harz mountains (Central Germany) as determined by FTIR, Pyrolysis-GC–MS and THM-GC–MS. *J. Anal. Appl. Pyrolysis* 126, 50–61. doi:10.1016/j.jaap.2017.06.025

Kaiser, K., and Kalbitz, K. (2012). Cycling downwards – dissolved organic matter in soils. *Soil Biol. biochem.* 52, 29–32. doi:10.1016/j.soilbio.2012.04.002

Kaiser, K., Guggenberger, G., Haumaier, L., and Zech, W. (2002). The composition of dissolved organic matter in forest soil solutions: changes induced by seasons and passage through the mineral soil. *Org. Geochem.* 33 (3), 307–318. doi:10.1016/S0146-6380(01)00162-0

Kaiser, K., Guggenberger, G., and Haumaier, L. (2004). Changes in dissolved lignin-derived phenols, neutral sugars, uronic acids, and amino sugars with depth in forested Haplic Arenosols and Rendzic Leptosols. *Biogeochemistry* 70, 135–151. doi:10.1023/B:BIOG.0000049340.77963.18

Kalbitz, K., Solinger, S., Park, J. H., Michalzik, B., and Matzner, E. (2000). Controls on the dynamics of dissolved organic matter in soils: a review. *Soil Sci.* 165 (4), 277–304. doi:10.1097/00010694-200004000-00001

Kalbitz, K., Schmerwitz, J., Schwesig, D., and Matzner, E. (2003). Biodegradation of soil-derived dissolved organic matter as related to its properties. *Geoderma* 113 (3-4), 273–291. doi:10.1016/S0016-7061(02)00365-8

Kalbitz, K., Schwesig, D., Rethemeyer, J., and Matzner, E. (2005). Stabilization of dissolved organic matter by sorption to the mineral soil. *Soil Biol. biochem.* 37 (7), 1319–1331. doi:10.1016/j.soilbio.2004.11.028

Kassambara, A., and Mundt, F. (2020). *Factoextra: extract and visualize the results of multivariate data analyses*. CRAN.

Kellerman, A. M., Kothawala, D. N., Dittmar, T., and Tranvik, L. J. (2015). Persistence of dissolved organic matter in lakes related to its molecular characteristics. *Nat. Geosci.* 8 (6), 454–457. doi:10.1038/ngeo2440

Kleber, M., Sollins, P., and Sutton, R. (2007). A conceptual model of organo-mineral interactions in soils: self-assembly of organic molecular fragments into zonal structures on mineral surfaces. *Biogeochemistry* 85, 9–24. doi:10.1007/s10533-007-9103-5

Kleber, M., Eusterhues, K., Keiluweit, M., Mikutta, C., Mikutta, R., and Nico, P. S. (2015). Mineral–organic associations: formation, properties, and relevance in soil environments. *Adv. Agron.* 130, 1–140. doi:10.1016/bs.agron.2014.10.005

Kothawala, D. N., Moore, T. R., and Hendershot, W. H. (2009). Soil properties controlling the adsorption of dissolved organic carbon to mineral soils. *Soil Sci. Soc. Am. J.* 73 (6), 1831–1842. doi:10.2136/sssaj2008.0254

Kothawala, D. N., Von Wachenfeldt, E., Koehler, B., and Tranvik, L. J. (2012). Selective loss and preservation of lake water dissolved organic matter fluorescence during long-term dark incubations. *Sci. Total Environ.* 433, 238–246. doi:10.1016/j.scitotenv.2012.06.029

Kothawala, D. N., Murphy, K. R., Stedmon, C. A., Weyhenmeyer, G. A., and Tranvik, L. J. (2013). Inner filter correction of dissolved organic matter fluorescence. *Limnol. Oceanogr. Methods* 11 (12), 616–630. doi:10.4319/lom.2013.11.616

Kramer, M. G., Sanderman, J., Chadwick, O. A., Chorover, J., and Vitousek, P. M. (2012). Long-term carbon storage through retention of dissolved aromatic acids by reactive particles in soil. *Glob. Change Biol.* 18 (8), 2594–2605. doi:10.1111/j.1365-2486.2012.02681.x

Krettek, A., and Rennert, T. (2021). Mobilisation of Al, Fe, and DOM from topsoil during simulated early Podzol development and subsequent DOM adsorption on model minerals. *Sci. Rep.* 11 (1), 19741. doi:10.1038/s41598-021-99365-y

Lê, S., Josse, J., and Husson, F. (2008). FactoMineR: an R package for multivariate analysis. *J. Stat. Softw.* 25 (1), 1–18. doi:10.18637/jss.v025.i01

Leinemann, T., Preusser, S., Mikutta, R., Kalbitz, K., Cerli, C., Höschen, C., et al. (2018). Multiple exchange processes on mineral surfaces control the transport of dissolved organic matter through soil profiles. *Soil Biol. biochem.* 118, 79–90. doi:10.1016/j.soilbio.2017.12.006

Li, J., Zhao, L., Li, M., Min, Y., Zhan, F., Wang, Y., et al. (2022). Changes in soil dissolved organic matter optical properties during peatland succession. *Ecol. Indic.* 143, 109386. doi:10.1016/j.ecolind.2022.109386

Lin, Y., Hu, E., Sun, C., Li, M., Gao, L., and Fan, L. (2023). Using fluorescence index (FI) of dissolved organic matter (DOM) to identify non-point source pollution: the difference in FI between soil extracts and wastewater reveals the principle. *Sci. Total Environ.* 862, 160848. doi:10.1016/j.scitotenv.2022.160848

Liu, Y., Ye, Q., Huang, W. L., Feng, L., Wang, Y. H., Xie, Z., et al. (2020). Spectroscopic and molecular-level characteristics of dissolved organic matter in the Pearl River Estuary, South China. *Sci. Total Environ.* 710, 136307. doi:10.1016/j.scitotenv.2019.136307

Liu, H., Xu, H., Wu, Y., Ai, Z., Zhang, J., Liu, G., et al. (2021). Effects of natural vegetation restoration on dissolved organic matter (DOM) biodegradability and its temperature sensitivity. *Water Res.* 191, 116792. doi:10.1016/j.watres.2020.116792

Liu, L., Gunina, A., Zhang, F., Cui, Z., and Tian, J. (2023). Fungal necromass increases soil aggregation and organic matter chemical stability under improved cropland

management and natural restoration. *Sci. Total Environ.* 858, 159953. doi:10.1016/j.scitotenv.2022.159953

Marschner, B., and Kalbitz, K. (2003). Controls of bioavailability and biodegradability of dissolved organic matter in soils. *Geoderma* 113 (3-4), 211–235. doi:10.1016/S0016-7061(02)00362-2

McKnight, D. M., Boyer, E. W., Westerhoff, P. K., Doran, P. T., Kulbe, T., and Andersen, D. T. (2001). Spectrofluorometric characterization of dissolved organic matter for indication of precursor organic material and aromaticity. *Limnol. Oceanogr.* 46 (1), 38–48. doi:10.4319/lo.2001.46.1.0038

Meng, Y., Li, P., Xiao, L., Hu, B., Zhang, C., Yang, S., et al. (2024). Differences in dissolved organic matter and analysis of influencing factors between plantations pure and mixed forest soils in the loess plateau. *Fron. For. Glob. Change* 7, 1344784. doi:10.3389/ffgc.2024.1344784

Moni, C., Rumpel, C., Virto, I., Chabbi, A., and Chenu, C. (2010). Relative importance of sorption versus aggregation for organic matter storage in subsoil horizons of two contrasting soils. *Eur. J. Soil Sci.* 61 (6), 958–969. doi:10.1111/j.1365-2389.2010.01307.x

Nannipieri, P., Angst, G., Mueller, C., and Pietramellara, G. (2025). The role of death and lysis of microbial and plant cells in the formation of soil organic matter. *Soil Biol. Biochem.* 204, 109750. doi:10.1016/j.soilbio.2025.109750

Nebbioso, A., and Piccolo, A. (2013). Molecular characterization of dissolved organic matter (DOM): a critical review. *Anal. Bioanal. Chem.* 405, 109–124. doi:10.1007/s00216-012-6363-2

Nieminen, T. M., De Vos, B., Cools, N., König, N., Fischer, R., Iost, S., et al. (2016). "Part XI: soil solution collection and analysis. Version 2016-2," in *UNECE ICP Forests Programme Co-ordinating Centre Manual on methods and criteria for harmonized sampling, assessment, monitoring and analysis of the effects of air pollution on forests* (Eberswalde, Germany: Thünen Institute of Forest Ecosystems), 20. Available online at: http://www.icp-forests.org/manual.htm.

O'Donnell, J. A., Aiken, G. R., Butler, K. D., Guillemette, F., Podgorski, D. C., and Spencer, R. G. (2016). DOM composition and transformation in boreal forest soils: the effects of temperature and organic-horizon decomposition state. *J. Geophys. Res. Biogeosciences* 121 (10), 2727–2744. doi:10.1002/2016JG003431

Ohno, T. (2002). Fluorescence inner-filtering correction for determining the humification index of dissolved organic matter. *Environ. Sci. Technol.* 36 (4), 742–746. doi:10.1021/es0155276

Oksanen, J., Blanchet, F. G., Friendly, M., Kindt, R., Legendre, P., McGlinn, D., et al. (2020). Vegan: community Ecology package. *R. package version* 2, 5–7. Available online at: https://CRAN.R-project.org/package=vegan.

Parlanti, E., Wörz, K., Geoffroy, L., and Lamotte, M. (2000). Dissolved organic matter fluorescence spectroscopy as a tool to estimate biological activity in a coastal zone submitted to anthropogenic inputs. *Org. Geochem.* 31 (12), 1765–1781. doi:10.1016/S0146-6380(00)00124-8

Perry, J. J., and Gibson, D. T. (1977). Microbial metabolism of cyclic hydrocarbons and related compounds. *Crit. Rev. Microbiol.* 5 (4), 387–412. doi:10.3109/10408417709102811

Pontiller, B., Martínez-García, S., Lundin, D., and Pinhassi, J. (2020). Labile dissolved organic matter compound characteristics select for divergence in marine bacterial activity and transcription. *Front. Microbiol.* 11, 588778. doi:10.3389/fmicb.2020.588778

Pucher, M., Wünsch, U., Weigelhofer, G., Murphy, K., Hein, T., and Graeber, D. (2019). staRdom: versatile software for analyzing spectroscopic data of dissolved organic matter in R. *Water* 11 (11), 2366. doi:10.3390/w11112366

Qin, X. Q., Yao, B., Jin, L., Zheng, X. Z., Ma, J., Benedetti, M. F., et al. (2020). Characterizing soil dissolved organic matter in typical soils from China using fluorescence EEM–PARAFAC and UV–visible absorption. *Aquat. Geochem.* 26, 71–88. doi:10.1007/s10498-019-09366-7

R Core Team (2024). *R: a language and environment for statistical computing*. R Foundation for Statistical Computing. Available online at: https://www.R-project.org/.

Roberts, D., Nachtegaal, M., and Sparks, D. L. (2005). "Speciation of metals in soils,". *Chemical processes in soils*. Editors M. A. Tabatabai and D. L. Sparks (Soil Science Society of America), 8, 619–654. doi:10.2136/sssabookser8.c13

Roth, V. N., Lange, M., Simon, C., Hertkorn, N., Bucher, S., Goodall, T., et al. (2019). Persistence of dissolved organic matter explained by molecular changes during its passage through soil. *Nat. Geosci.* 12 (9), 755–761. doi:10.1038/s41561-019-0417-4

Schulten, H. R., and Schnitzer, M. (1997). Chemical model structures for soil organic matter and soils. *Soil Sci.* 162 (2), 115–130. doi:10.1097/00010694-199702000-00005

Seifert, A. G., Roth, V. N., Dittmar, T., Gleixner, G., Breuer, L., Houska, T., et al. (2016). Comparing molecular composition of dissolved organic matter in soil and stream water: influence of land use and chemical characteristics. *Sci. Total Environ.* 571, 142–152. doi:10.1016/j.scitotenv.2016.07.033

Singh, S., Dash, P., Silwal, S., Feng, G., Adeli, A., and Moorhead, R. J. (2017). Influence of land use and land cover on the spatial variability of dissolved organic matter in multiple aquatic environments. *Environ. Sci. Pollut. Res.* 24 (16), 14124–14141. doi:10.1007/s11356-017-8917-5

Sokol, N. W., and Bradford, M. A. (2019). Microbial formation of stable soil carbon is more efficient from belowground than aboveground input. *Nat. Geosci.* 12 (1), 46–53. doi:10.1038/s41561-018-0258-6

Stedmon, C. A., and Bro, R. (2008). Characterizing dissolved organic matter fluorescence with parallel factor analysis: a tutorial. *Limnol. Oceanogr. Methods* 6 (11), 572–579. doi:10.4319/lom.2008.6.572

Steinbeiss, S., Temperton, V. M., and Gleixner, G. (2008). Mechanisms of short-term soil carbon storage in experimental grasslands. *Soil Biol. biochem.* 40 (10), 2634–2642. doi:10.1016/j.soilbio.2008.07.007

Tfaily, M. M., Hamdan, R., Corbett, J. E., Chanton, J. P., Glaser, P. H., and Cooper, W. T. (2013). Investigating dissolved organic matter decomposition in northern peatlands using complimentary analytical techniques. *Geochim. Cosmochim. Acta* 112, 116–129. doi:10.1016/j.gca.2013.03.002

Tian, J., Zong, N., Hartley, I. P., He, N., Zhang, J., Powlson, D., et al. (2021). Microbial metabolic response to winter warming stabilizes soil carbon. *Glob. Change Biol.* 27 (10), 2011–2028. doi:10.1111/gcb.15538

Tian, S., Zhu, S., Kaal, J., Lv, J., Huang, R., Zhang, T., et al. (2025). Does greater molecular diversity in soil organic matter imply greater persistence: Insights from molecular and multi-property analyses in Western China. *Geochim. Cosmochim. Acta* 401, 136–148. doi:10.1016/j.gca.2025.06.008

Tong, H., Simpson, A. J., Paul, E. A., and Simpson, M. J. (2021). Land-use change and environmental properties alter the quantity and molecular composition of soil-derived dissolved organic matter. *ACS Earth Space Chem.* 5 (6), 1395–1406. doi:10.1021/acsearthspacechem.1c00033

Wagai, R., Kajiura, M., and Asano, M. (2020). Iron and aluminum association with microbially processed organic matter via meso-density aggregate formation across soils: organo-metallic glue hypothesis. *SOIL* 6 (2), 597–627. doi:10.5194/soil-6-597-2020

Wang, H., Richardson, C. J., and Ho, M. (2015). Dual controls on carbon loss during drought in peatlands. *Nat. Clim. Change* 5 (6), 584–587. doi:10.1038/nclimate2643

Weishaar, J. L., Aiken, G. R., Bergamaschi, B. A., Fram, M. S., Fujii, R., and Mopper, K. (2003). Evaluation of specific ultraviolet absorbance as an indicator of the chemical composition and reactivity of dissolved organic carbon. *Environ. Sci. Technol.* 37 (20), 4702–4708. doi:10.1021/es030360x

Xenopoulos, M. A., Barnes, R. T., Boodoo, K. S., Butman, D., Catalán, N., D'Amario, S. C., et al. (2021). How humans alter dissolved organic matter composition in freshwater: relevance for the Earth's biogeochemistry. *Biogeochemistry* 154, 323–348. doi:10.1007/s10533-021-00753-3

Xu, Z., and Tsang, D. C. (2024). Mineral-mediated stability of organic carbon in soil and relevant interaction mechanisms. *Eco-Environment Health* 3 (1), 59–76. doi:10.1016/j.eehl.2023.12.003

Xu, L., Hu, Q., Jian, M., Mao, K., Liu, Z., Liao, W., et al. (2023). Exploring the optical properties and molecular characteristics of dissolved organic matter in a large river-connected lake (Poyang Lake, China) using optical spectroscopy and FT-ICR MS analysis. *Sci. Total Environ.* 879, 162999. doi:10.1016/j.scitotenv.2023.162999

Xue, S., Zhao, Q., Wei, L., Song, Y., and Tie, M. (2013). Fluorescence spectroscopic characterization of dissolved organic matter fractions in soils in soil aquifer treatment. *Environ. Monit. Assess.* 185, 4591–4603. doi:10.1007/s10661-012-2890-8

Yang, Z., Ohno, T., and Singh, B. (2024). Effect of land use change on molecular composition and concentration of organic matter in an Oxisol. *Environ. Sci. Technol.* 58 (23), 10095–10107. doi:10.1021/acs.est.4c00740

Zhang, Y., Wang, X., Wang, X., and Li, M. (2019). Effects of land use on characteristics of water-extracted organic matter in soils of arid and semi-arid regions. *Environ. Sci. Pollut. Res.* 26 (25), 26052–26059. doi:10.1007/s11356-019-05858-9